

## Motivation



Cat's Eye Nebula NGC 6543

Over the last years the investigation of complex (dusty) macroscopic and mesoscopic plasmas occurring e.g. in astrophysical, laboratory and technical situations has become an important research field. The theoretical description of complex plasmas is extremely difficult due to their heterogeneous composition and the drastic differences in the relevant space and times scales [1, 2].

With the help of confinement potentials it has become possible to trap, for long periods of time, plasmas of a single charge (non-neutral plasmas). By varying the confinement strength researchers have achieved liquid behavior and even Coulomb crystallization of ions [3] and dust particles [4, 5]. These strong correlation phenomena are of exceptional current interest.

This contribution deals with the simulation and analysis of spherically 3D clusters which were recently first experimentally observed in dusty plasmas [6]. We compare simulation results to real dust clusters from experiments. In the simulations the dust-dust interaction potential is modelled by a Coulomb/Yukawa potential [7].

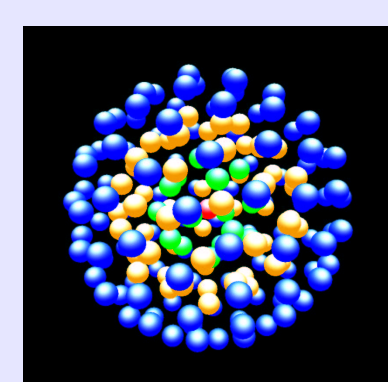
## Model

We consider  $N$  classical particles with equal charge  $q$  and mass  $m$  interacting via a statically screened Coulomb potential (Yukawa), where  $\kappa$  is the inverse screening length, and being confined in a 3D isotropic harmonic trap with frequency  $\omega$  with the hamiltonian

$$H_N = \sum_{i=1}^N \frac{m}{2} \dot{r}_i^2 + \sum_{i=1}^N \frac{m}{2} \omega^2 r_i^2 + \sum_{i>j}^N \frac{q^2 \exp(-\kappa|\mathbf{r}_i - \mathbf{r}_j|)}{4\pi\epsilon|\mathbf{r}_i - \mathbf{r}_j|}$$

Below we will use dimensionless lengths and energies by introducing the units  $r_0 = (q^2/2\pi\epsilon m \omega^2)^{1/3}$  and  $E_0 = (m\omega^2 q^4/32\pi^2\epsilon^2)^{1/3}$ , respectively.

## Shell Structure, Cluster Stability and Symmetry



At zero temperature (zero particle velocities  $\dot{r}_i$ , infinite coupling) concentric shells are observed with characteristic closures as well as *magic* clusters. The stability of clusters is characterized by the *binding energy* (addition energy change) [8]:

$$\Delta_2(N) = E(N+1) + E(N-1) - 2E(N).$$

Further, the symmetry within the shells can be analyzed by performing a Voronoi analysis, i.e. by constructing polygons around a given particle formed by the lines equally bisecting nearest-neighbor pairs on the shell. To quantify this topological criterion, we introduce the *Voronoi symmetry parameter*

$$G_M = \frac{1}{N_M} \sum_{j=1}^{N_M} \frac{1}{M} \left| \sum_{k=1}^M e^{iM\theta_{jk}} \right|,$$

where  $N_M$  denotes the number of particles in the shell, each of which is surrounded by a Voronoi polygon of order  $M$ , ( $M$  nearest neighbors) and  $\theta_{jk}$  is the angle between the  $j$ -th particle and its  $k$ -th nearest neighbor. A value  $G_5 = 1$  ( $G_6 = 1$ ) means that all pentagons (hexagons) are perfect, the reduction of  $G_M$  below 1 is a measure of their distortion.

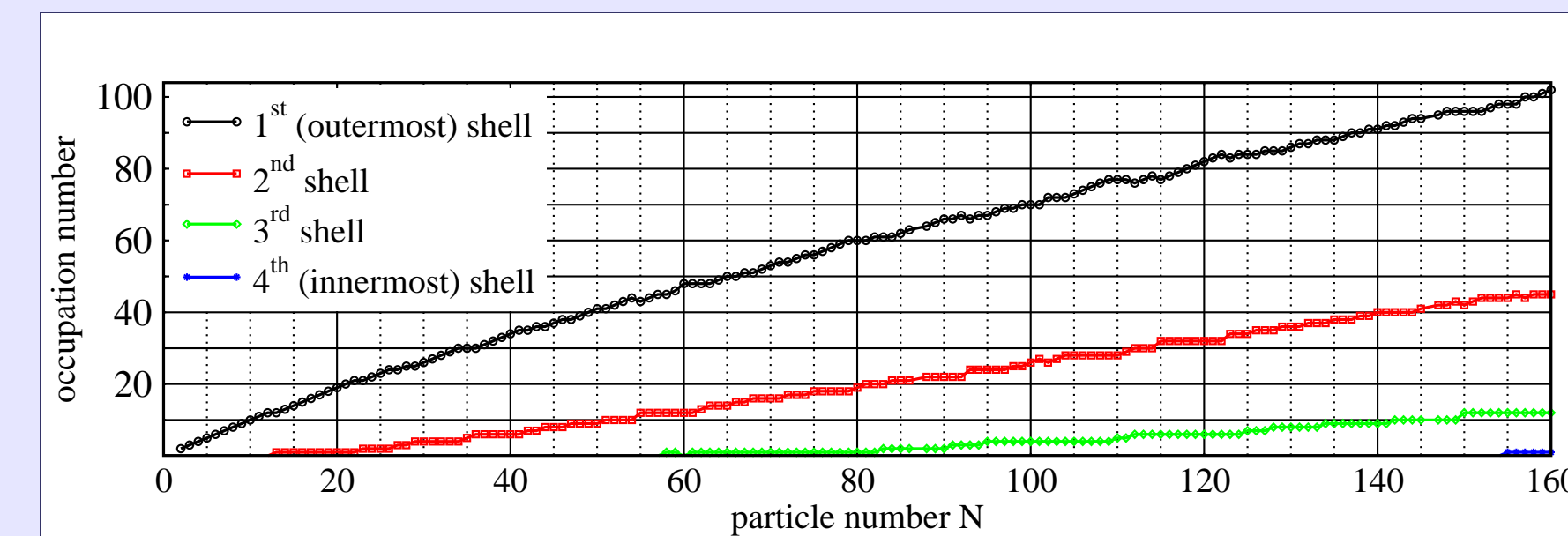
Now it is easy to define the *mean Voronoi symmetry parameter* (MVSP)  $\langle G^{(s)} \rangle$  to quantify the symmetry of the  $s$ -th shell of the cluster

$$\langle G^{(s)} \rangle = \frac{1}{N_s} \sum_M N_M G_M^{(s)},$$

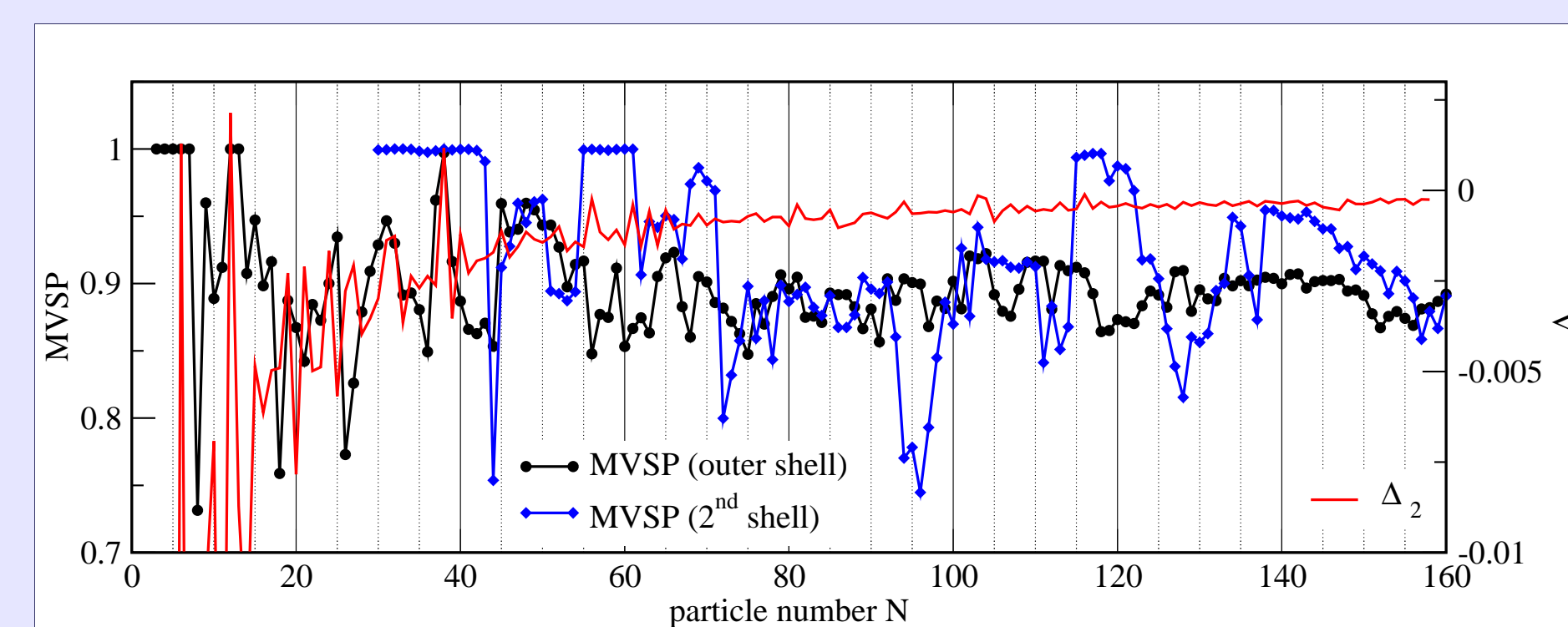
where  $N_s$  denotes the number of all particles in shell  $s$ .

## Simulation – Coulomb Clusters ( $\kappa = 0$ )

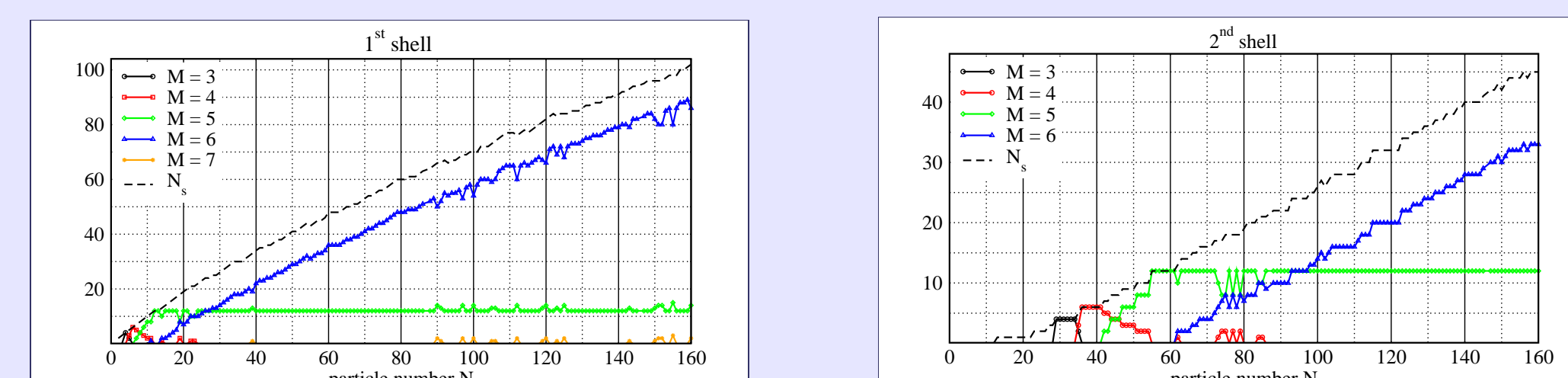
### Analysis of 3D Coulomb Clusters



Number of particles  $N_s$  on shell  $s$  vs.  $N$ . Note the recurrence of two shells at  $N = 60$ . The 2<sup>nd</sup> shell is opened at  $N = 13$ , the 3<sup>rd</sup> shell at  $N = 58$  (and  $N = 61$ ), the 4<sup>th</sup> shell at  $N = 155$ .



Binding energy  $\Delta_2$  and MVSP of the two outermost shells vs. particle number  $N$ . Magic clusters are  $N = 4, 6, 10, 12, 19, 32, 38, 56$  [8] and  $N = 81, 94, 103, 116$  [7].



Number  $N_M$  of Voronoi polygons with  $M$  edges in the two outermost shells vs.  $N$ .

### Fine structure

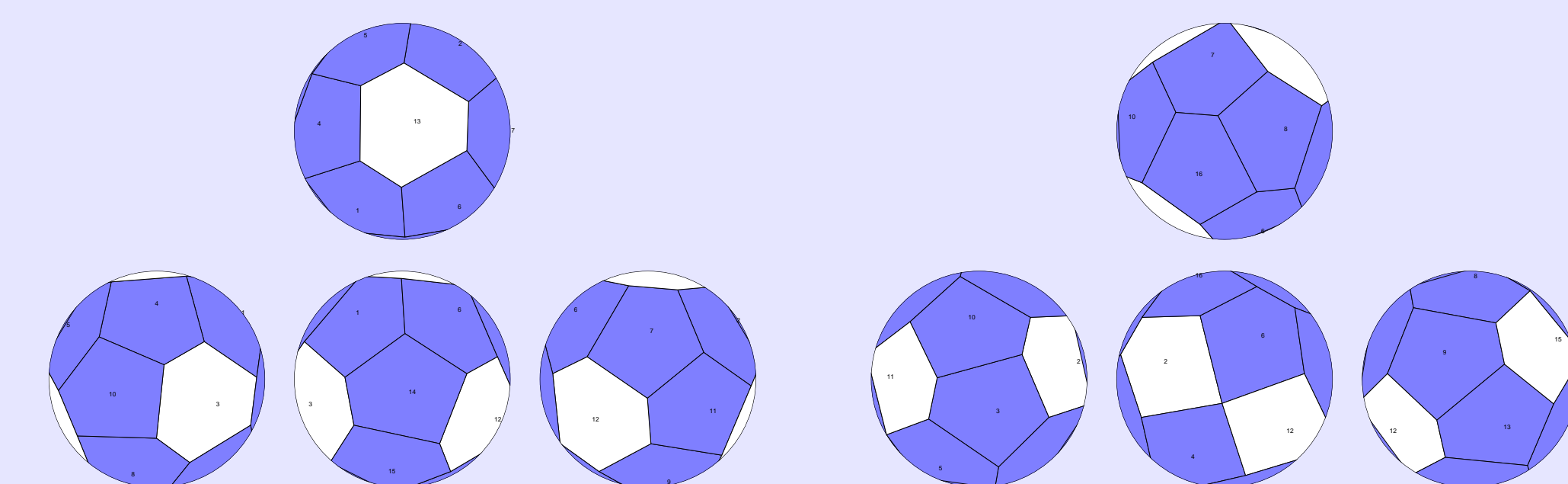
Between ground state and excited states with different shell configurations meta-stable states exist which differ only in the intra-shell symmetry.

### Ground state (16,1)

$$\begin{aligned} E/N &= 6.388610 \\ r_1 &= 1.5042 \\ G_5 &= 0.891 \quad [12x] \\ G_6 &= 0.993 \quad [4x] \\ \langle G^{(1)} \rangle &= 0.916 \end{aligned}$$

### First meta-stable state (16,1)

$$\begin{aligned} E/N &= 6.388975 \\ r_1 &= 1.5042 \\ G_5 &= 0.746 \quad [12x] \\ G_6 &= 0.884 \quad [4x] \\ \langle G^{(1)} \rangle &= 0.781 \end{aligned}$$

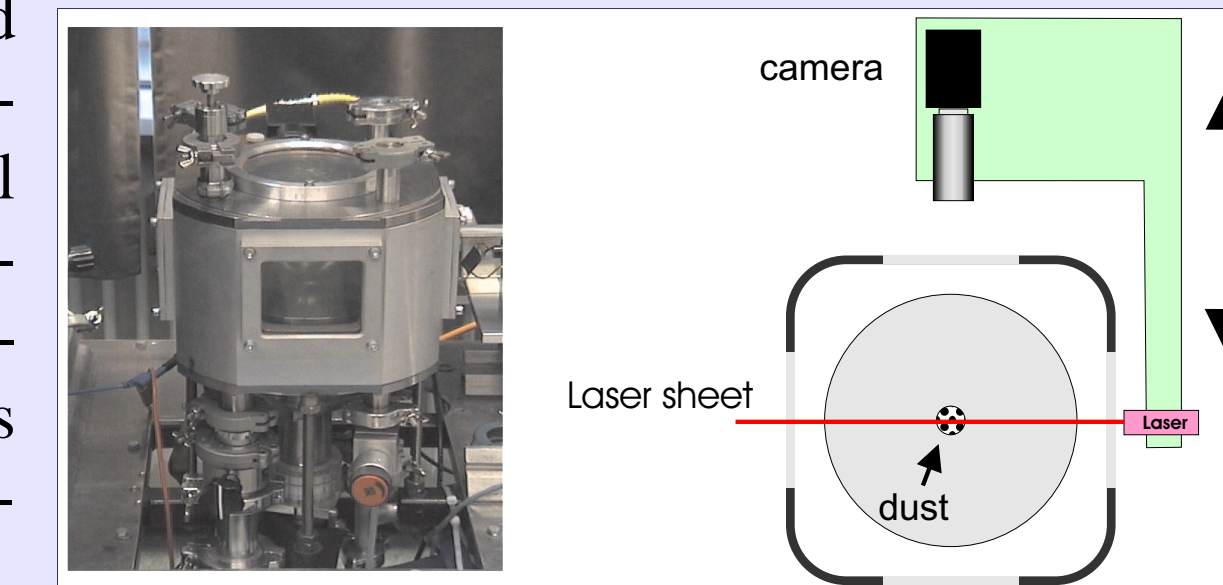


Ground state and first meta-stable state of  $N = 17$  have identical shell configuration and number of Voronoi polygons (numbers in brackets). These states differ, however, in the arrangement of the polygons – compare arrangement of the four bright hexagons also denoted by A, B, C, and D in the left figure. In the meta-stable state, axis A-B is rotated. At the same time, the symmetry ( $G_5, G_6$ ) is reduced.

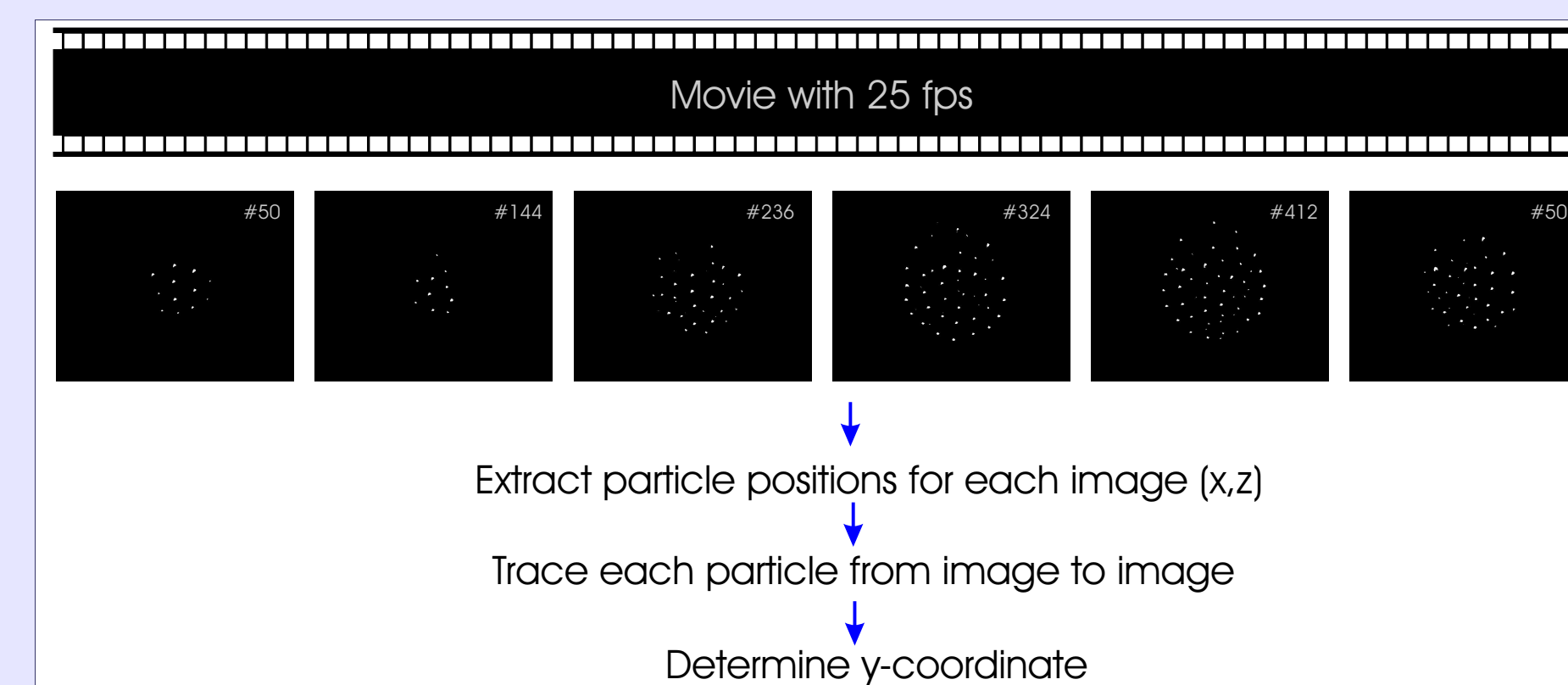
## Experiment

### Setup

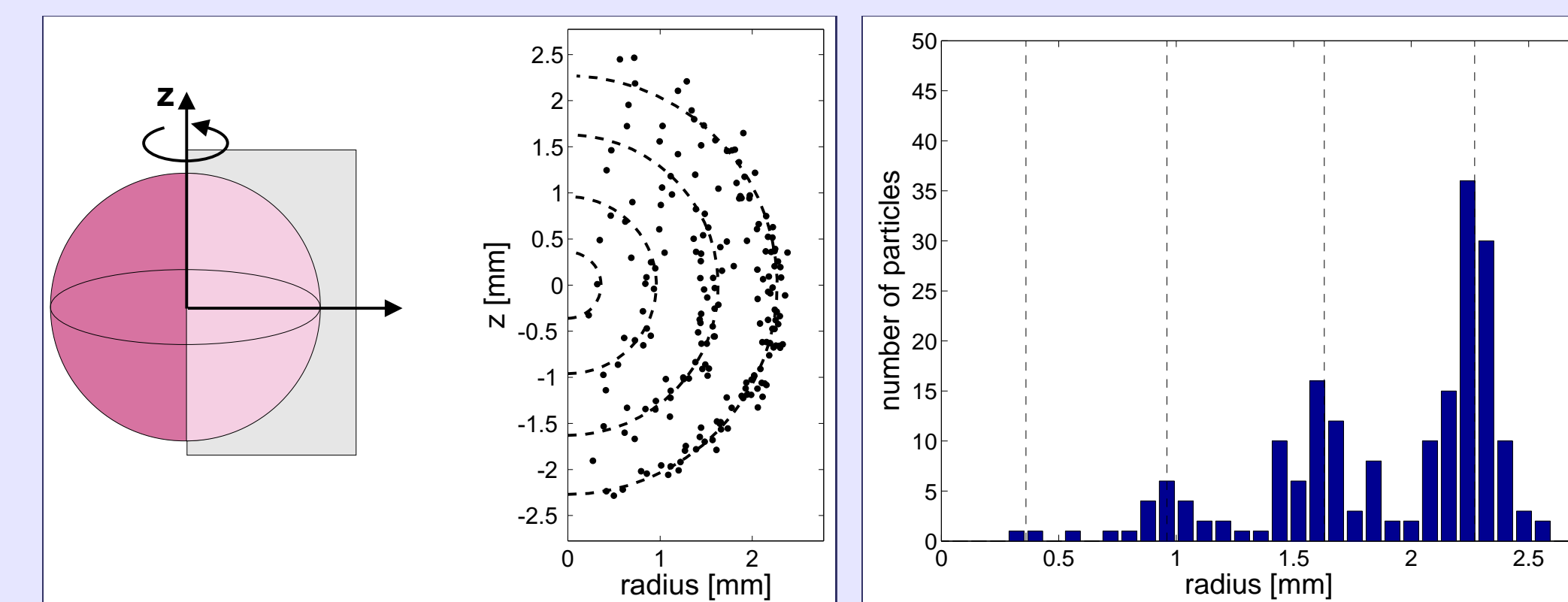
The experiments are performed in a capacitively coupled rf-discharge in argon. Typical parameter are: vertical temperature gradient  $5 \text{ K cm}^{-1}$ , rf-power below 30 W, neutral gas pressure 50-150 Pa, particle diameter  $3.4 \mu\text{m}$ .



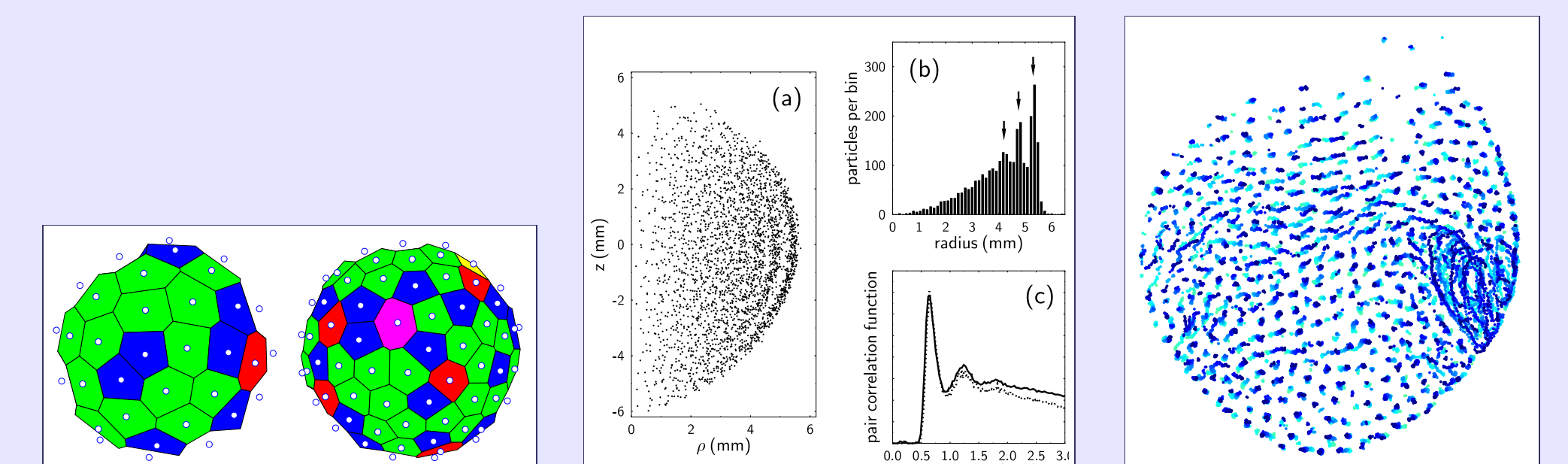
### Data Analysis



## Results



Particle cluster with 190 particles, shell occupation: 2, 21, 60, 107, inter-shell distance: 0.63 mm, inter-particle distance: 0.715 mm.



Particles arrange in nested shell! Crystalline order on shells!

Larger particle clouds show shell formation only close to surface ( $N = 2800$ ).

At the solid-fluid phase transition ( $N = 6000$ ).

## Conclusions

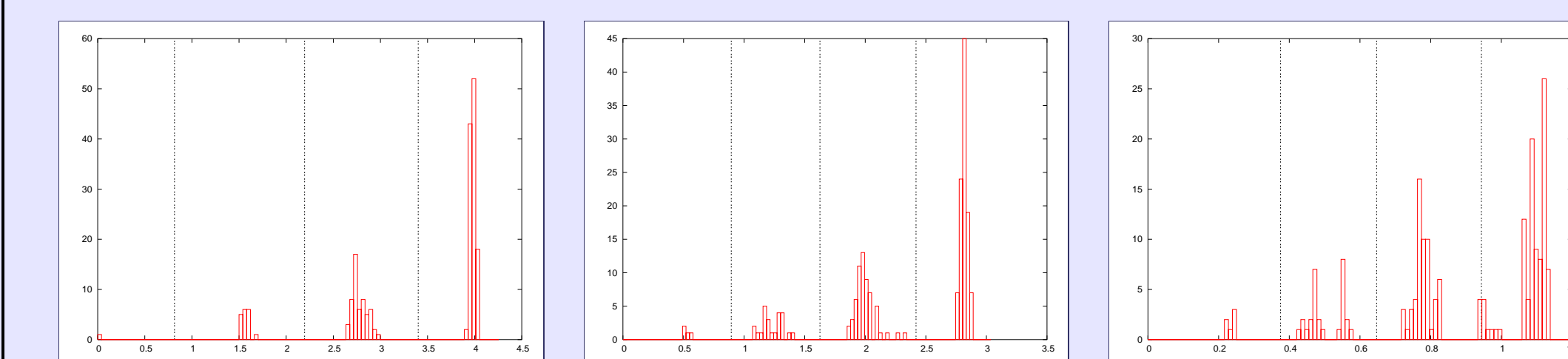
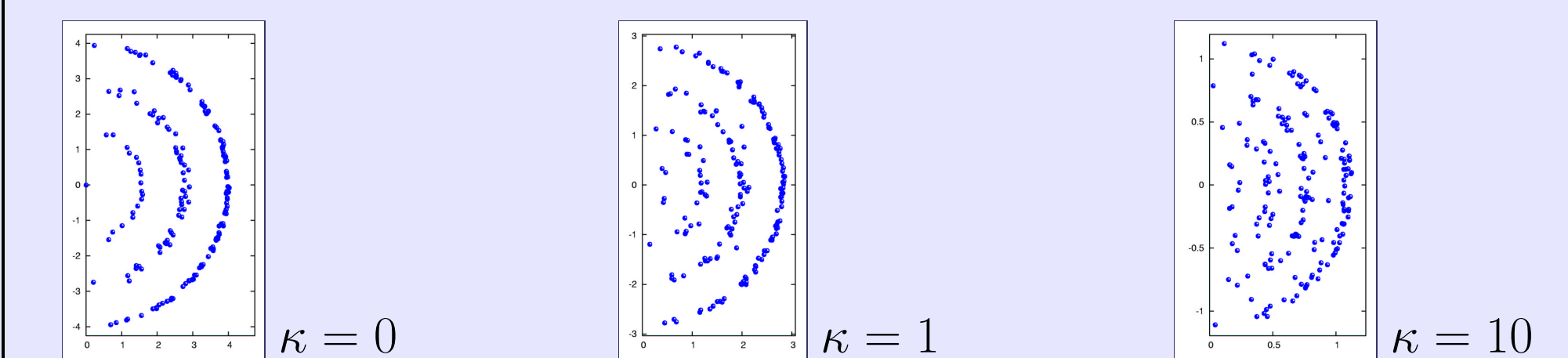
- Observation of spherical, crystalline, void-free dust clouds under laboratory conditions.
- First evidence for structural changes with increasing cluster size.
- First evidence of dynamic and thermodynamic effects.

## Simulation – Yukawa Cluster ( $\kappa > 0$ )

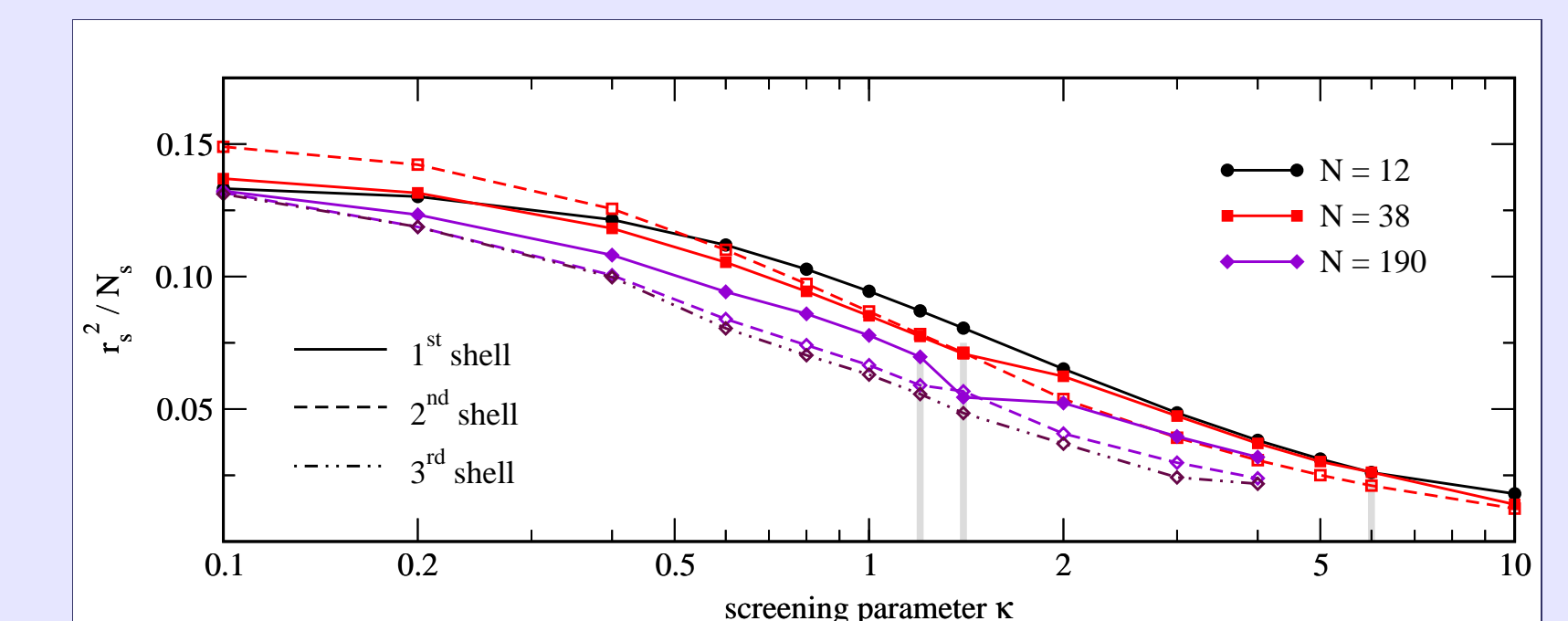
### Effects of screening on shell structure

In the following the plot of the vertical vs. the radial position of the particles is shown for three different values of screening (upper figures). In addition the histogram of the cluster is plotted (lower figures), in comparison to experiments.

### I) Increase of shell width with $\kappa$



### II) Reduction of shell radii



Square of (normalized) shell radii vs. screening parameter  $\kappa$  for  $N = 12, 38, 190$ .

### III) Change of shell configuration

$\kappa$	Configuration	E/N
0.0	(115,56,18,1)	36.357
0.2	(114,57,18,1)	23.729
0.4	(110,58,20,2)	17.608
0.6	(107,60,21,2)	14.028
0.8	(105,60,22,3)	11.672
1.0	(102,60,24,4)	9.998

Continuous increase of particle number on inner shells with  $\kappa$ . No reversal of this trend is observed as in 2D ( $N = 190$ ).

### IV) Screening induced structural change from shell configuration to bulk-like symmetry.

The comparison of experiments with theory shows: MD-simulations with a Yukawa potential as dust-dust interaction at  $\kappa \approx 0.6$  quantitatively reproduce experimental configurations.

## References

- [1] G.E. Morfill and H. Kersten, New J. Phys. **5** (2003).
- [2] D.H.E. Dubin and T.M. O'Neill, Rev. Mod. Phys. **71**, 87 (1999).
- [3] W.M. Itano, J.J. Bollinger, J.N. Tan, B. Jelenkovic, and D.J. Wineland, Science **297**, 686 (1998).
- [4] H. Thomas, G.E. Morfill, V. Demmel, J. Goree, B. Feuerbacher, and D. Möhlmann, Phys. Rev. Lett. **73**, 652 (1994).
- [5] Y. Hayashi, and K. Tachibana, Jpn. J. Appl. Phys. **33**, L804 (1994).
- [6] O. Arp, D. Block, A. Melzer, and A. Piel, Phys. Rev. Lett., accepted (2004).
- [7] P. Ludwig, S. Kosse, and M. Bonitz, submitted to Phys. Rev. E (2004); arXiv:physics/0409095; arXiv:physics/0409100.
- [8] K. Tsuruta and S. Ichimaru, Phys. Rev. A **48**, 1339 (1993).